JOURNAL OF BAKU ENGINEERING UNIVERSITY - PHYSICS
2025. Volume 9, Number 1 *Pages 35-42*

UDC 535.34:537.311.33
DOI: https://doi.org/10.30546/09081.2025.001.8005

ABSORPTION AND BAND STRUCTURE MODIFICATION IN BORON-SUBSTITUTED GaSe

Lamiya BALAYEVA[1*], Ali GUSEINOV[2]

[1]*Department of Semiconductor physics,*
Baku State University,
Baku, Azerbaijan
[2]*Department of Semiconductor physics,*
Baku State University,
Baku, Azerbaijan

ARTICLE INFO

Article history
Received:2025-09-29
Received in revised form:2025-11-06
Accepted:2025-11-18
Available online

Keywords:
Optical properties,
Layered chalcogenide semiconductors,
Band gap narrowing,
Electronic band structure modification,
Visible and near – infrared photodetection

ABSTRACT

Single crystals $Ga_{1-x}B_xSe$ *(x = 0.3 and 0.5%) were synthesized using the horizontal Bridgman method, and their optical characteristics were systematically examined. UV–Vis absorption spectra revealed a direct band gap of 1.960–1.963 eV, slightly narrower than that of undoped GaSe (≈ 2.0 eV). This reduction originates from lattice distortions and electronic perturbations introduced by boron atoms, which shift the absorption edge toward longer wavelengths, improving the material's suitability for visible and near-infrared photodetection. Additional absorption features at 1.05 eV and 1.35 eV correspond to boron-induced impurity states that affect the temperature dependence of absorption. At lower boron concentrations, the absorption coefficient increases with temperature due to thermal excitation, while at higher concentrations, a negative temperature coefficient appears, indicating enhanced radiative recombination. These results demonstrate that controlled boron incorporation effectively tailors the band structure and optical response of GaSe, enabling its application in broadband optoelectronic and photodetector devices.*

[*] Corresponding author.*E-mail addresses*: *blamiye99@gmail.com (Lamiya Balayeva).*

1. Introduction

Gallium selenide (GaSe) is a III–VI semiconductor with a layered structure that crystallizes in four distinct polymorphic forms: β, γ, δ, and ε [1]. Among these, ε–GaSe is of particular significance due to its diverse optical applications. Devices based on ε–GaSe include photodetectors [2–4], phototransistors [5,6], energy storage systems [7], and nonlinear optical applications [8–10]. Furthermore, the bandgap of ε–GaSe can be tuned either by applying external strain or by reducing its thickness to a few layers [11–16], thereby opening up new opportunities for the development of next-generation devices [11,17]. The epitaxial properties of ε–GaSe also enable compatibility with other two-dimensional (2D) materials, facilitating the fabrication of ultrathin heterojunctions and their subsequent application in various optoelectronic devices [8,18]. More broadly, chalcogenides such as GaSe are highly attractive for non-resonant applications owing to their strong nonlinear optical response and large real refractive index [19]. In addition, the high absorption coefficient of GaSe makes it suitable as a

light-absorbing material in solar cells. Thus, the study of its optical parameters is of particular importance, as it provides a deeper understanding of the material's optical quality.

In general, to achieve a comprehensive understanding of the optical and electronic behavior of any material, parameters such as the refractive index (n), extinction coefficient (k), absorption coefficient (α), and band structure characteristics are essential. Specifically, accurate determination of the wavelength dependence of the complex refractive index N(λ) and the complex dielectric function $\varepsilon(\lambda)$ yields critical insights into the dispersion and absorption features of the material, which are crucial for its implementation in optoelectronic devices [20,21]. It should be noted that these fundamental optical parameters are related not only to $\alpha(\lambda)$ but also to the reflectance R(λ). However, precise determination of R(λ) remains an open issue that requires particular attention. Moreover, in many cases, the computational methods employed provide reliable results only within the transparency region [22–26]; outside this range, inaccuracies may arise, potentially leading to misinterpretation of experimental results.

Considering these aspects, the determination of the optical parameters of $Ga_{1-x}B_xSe$ (x = 0.3, 0.5%) crystals synthesized by us is of great significance, both for obtaining comprehensive information about these crystals and for identifying their potential application areas. For this reason, in the present work, a solid solution $Ga_{1-x}B_xSe$ was synthesized by substituting part of the gallium (Ga) atoms with boron (B) atoms. The grown single crystals were then investigated in detail to determine their optical parameters.

2. Experimental details

2.1. Growing of $Ga_{1-x}B_xSe$ crystals

The $Ga_{1-x}B_xSe$ solid solution was synthesized in evacuated quartz ampoules through direct melting of the constituent elements, with a total mass of 15 g. The reaction proceeded via an exothermic pathway. To mitigate excessive pressure accumulation within the ampoule, one end of the sealed tube was externally cooled, while the opposite end was gradually heated in an electric furnace to 1100 °C. Upon completion of the initial reaction, the ampoule was transferred to an isothermal furnace maintained at 1100 °C and subjected to an annealing process lasting 4 h, thereby ensuring compositional homogenization. The resulting ingot displayed uniform chemical composition and was characterized by the presence of large crystalline domains. This ingot was subsequently ground into a fine powder and reloaded into a quartz ampoule. After evacuation to a residual pressure of 10^{-5} Pa, the ampoule was hermetically sealed and utilized for single-crystal growth employing the horizontal Bridgman technique. Macroscopic examination of the as-grown crystals revealed a dark-red coloration accompanied by a distinct layered morphology, features that are typical of GaSe-based compounds.

2.2. Characterization techniques

The photoelectric characteristics of the samples were examined under high-vacuum conditions using a closed-cycle cryostat system. This setup enabled comprehensive measurements across a broad temperature range from 110 K to 400 K and within the optical spectral range of 480–2000 nm, facilitating the investigation of temperature-dependent carrier transport and spectral response behavior.

The optical characteristics of the samples were further examined using a Specord 250 Plus UV–Vis spectrophotometer across the spectral range of 190–1100 nm, providing comprehensive insight into their absorption behavior.

3. Result and discussions

Figure 1(a) presents the absorption spectrum of the $Ga_{0.997}B_{0.003}Se$ crystal at room temperature. As can be seen, a pronounced absorption edge appears around 650 nm. Beyond this threshold, the absorption intensity decreases sharply with increasing wavelength and becomes nearly constant above approximately 700 nm. Such behavior is characteristic of a material possessing a direct band gap. Figure 1(b) illustrates the dependence of $(\alpha h\nu)^2$ on $h\nu$, from which the band gap was determined using the Tauc method. Analysis yielded a band gap energy of approximately 1.963 eV, which is slightly lower than the well-established value for pure GaSe (≈ 2.0 eV [27]). This reduction is attributed to the partial substitution of Ga atoms by B atoms. The smaller atomic radius of boron introduces local lattice distortions, leading to subtle modifications in the electronic energy levels and, consequently, a narrowing of the band gap. The band gap narrowing effectively extends the optical absorption range of GaSe towards longer wavelengths. This property is particularly advantageous for photodetector applications operating in the visible and near-infrared (NIR) spectral regions. Importantly, the sharpness of the absorption edge is preserved upon boron incorporation, indicating the high crystalline quality of the material. Thus, the controlled introduction of boron offers a viable means of tuning the spectral sensitivity of GaSe-based optoelectronic devices.

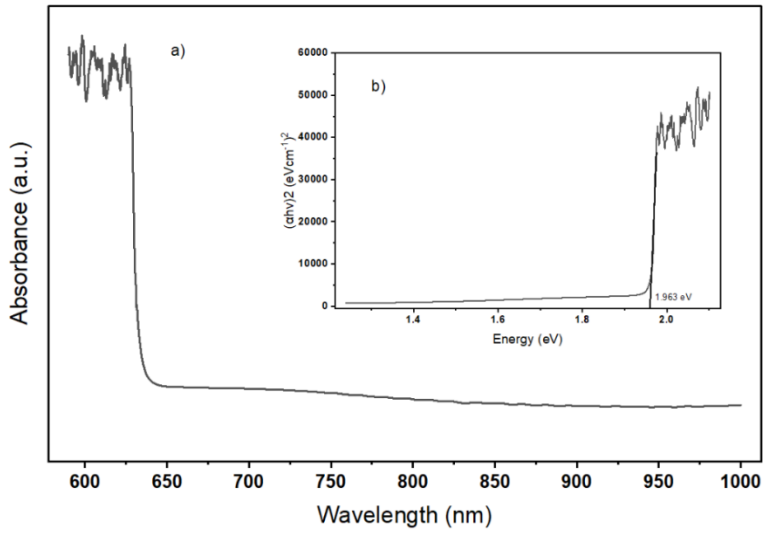

Fig. 1. (a) Absorption spectrum of the $Ga_{0.997}B_{0.003}Se$ crystal and (b) determination of the band gap energy based on the Tauc dependence.

Figure 2 presents the absorption spectra of a 120 μm thick $Ga_{0.997}B_{0.003}Se$ thin film measured at 300 K and 110 K. The spectra correspond to the long-wavelength edge of the intrinsic absorption band. Two distinct spectral features are observed at photon energies of approximately 1.05 eV and 1.35 eV. As reported in [28], the incorporation of boron atoms into GaSe crystals introduces impurity levels located at a depth of 1.05 eV. Given the layered structure of GaSe, it is most plausible that the boron atoms occupy interlayer positions. Nevertheless, under partial substitution of Ga atoms in the stoichiometric lattice of gallium selenide, boron atoms may also reside at vacant gallium sites, thereby engaging in chemical bonding with both selenium and gallium atoms. The optical transitions detected at an energy of 1.05 eV can reasonably be attributed to electron transitions from the $4P_1$ level of Ga (5.999 eV) to the $3S_2S_1/_2$ level of B (4.9663 eV). This interpretation supports the role of boron incorporation in modifying the electronic structure of GaSe and establishing localized impurity states within the band gap.

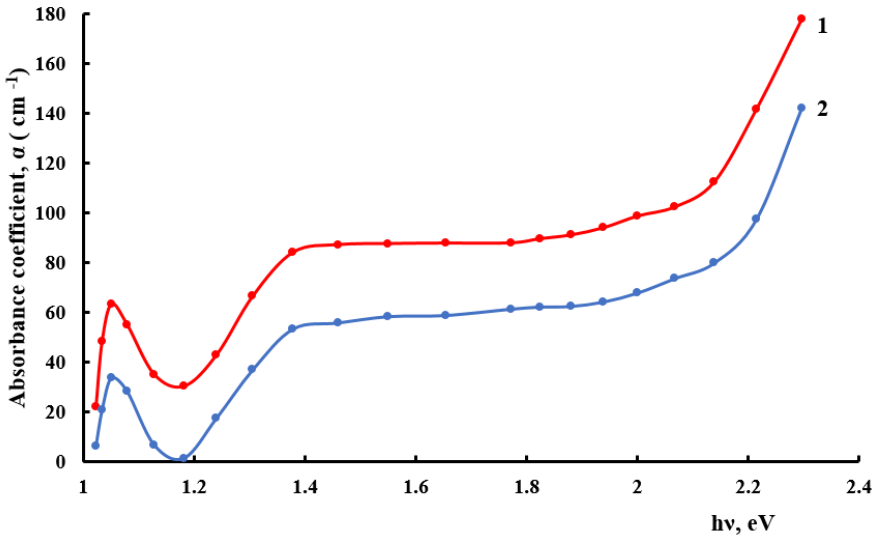

Fig. 2. Absorption spectra of the $Ga_{0.997}B_{0.003}Se$ crystal at 300 K (1) and 110 K (2)

The $Ga_{0.997}B_{0.003}Se$ crystals exhibit p-type conductivity, similar to that of pure GaSe. The optical absorption feature observed at 1.35 eV is most likely associated with electronic transitions from the acceptor level to the conduction band. The impurity-band absorption spectrum for a parabolic dispersion is described by the following expression [29]:

$$\alpha(h\vartheta) = \frac{32\pi e^2\hbar^2}{n_0 m_0}\,\frac{\varepsilon_{eff}}{\varepsilon}\,\left|\vec{e}\vec{P}_{cv}\right|\frac{m_e^*}{m_r R^*}\cdot\frac{S\,(\nu,x)}{h\nu}\,N_i F_{AB}$$

where n0 is the refractive index; $\frac{\varepsilon_{eff}}{\varepsilon}$ is the correction for the effective field, taking into account the dependence of the field in the crystal on its polarization; me* is the effective mass in the conduction band; mr is the reduced mass of an electron and a hole; R* is the effective Rydberg constant; (S (ν,x))/hν is the flux of photons with energy hν; Ni is the impurity concentration; FAB is the probability that the initial state is occupied and the final state is free. As the equation indicates, the absorption coefficient is strongly dependent on the concentration of electrons localized at the acceptor level. With increasing temperature, the population of these states rises due to thermal excitation of valence-band electrons into acceptor states, which in turn enhances the absorption coefficient. This temperature dependence is evident in Figure 1, where the absorption coefficient of $Ga_{0.997}B_{0.003}Se$ increases with rising temperature, indicating a positive temperature coefficient of absorption.

Figure 3(a) shows the absorption spectrum of the $Ga_{0.995}B_{0.005}Se$ crystal at T = 300 K. The absorption edge is clearly observed in the 635–650 nm interval. As the wavelength increases, the absorption decreases and becomes nearly constant beyond 700 nm. Figure 3(b) presents the Tauc plot, $(\alpha h\nu)^2$ on hν. From this analysis, the band gap energy was estimated to be approximately 1.960 eV. This value is very close to that obtained for the $Ga_{0.993}B_{0.003}Se$ crystal (≈ 1.963 eV) and slightly smaller than that of pure GaSe (≈ 2.0 eV). The results indicate that increasing the boron concentration does not lead to abrupt changes in the band gap but instead produces a gradual narrowing. This effect can be explained by local lattice distortions and modifications of electronic energy levels arising from the substitution of Ga atoms with smaller-radius B atoms. The

observed narrowing of the band gap suggests that the incorporation of boron allows for the spectral range of GaSe-based optoelectronic devices to extend towards the near-infrared region, thereby improving their applicability in broadband photodetection.

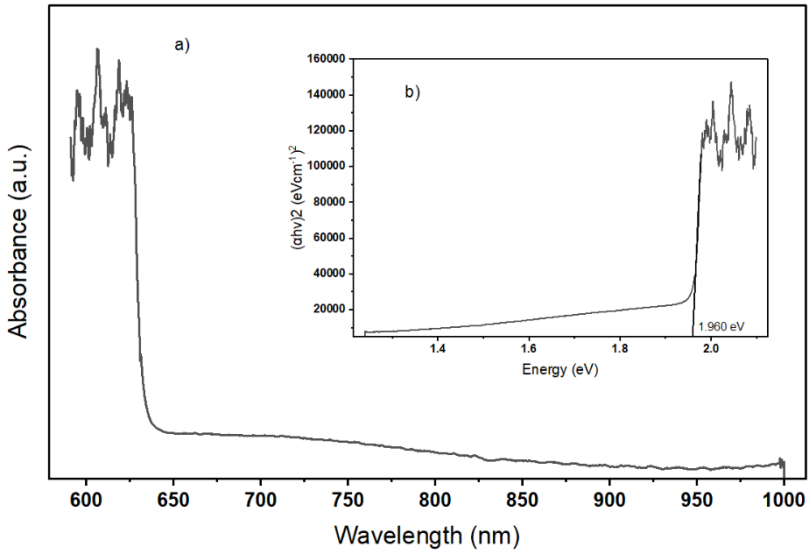

Fig. 3. (a) Absorption spectrum of the $Ga_{0.995}B_{0.005}Se$ crystal and (b) determination of the band gap energy based on the Tauc dependence.

The absorption coefficient spectrum of the $Ga_{0.995}B_{0.005}Se$ crystal at the long-wavelength edge of the fundamental absorption band exhibits a similar overall character to that of the previously studied spectrum (Fig. 4). However, in the $Ga_{0.995}B_{0.005}Se$ crystal, the absorption coefficient in the region around 1.05 eV is noticeably lower compared to the corresponding value in $Ga_{0.997}B_{0.003}Se$. Furthermore, in contrast to the earlier case, the temperature absorption coefficient of the $Ga_{0.995}B_{0.005}Se$ crystal assumes a negative sign. When the temperature is increased from 110 K to 300 K, the photoluminescence (PL) intensity of the crystals shows a slight enhancement. This observation suggests that the negative temperature dependence of the absorption coefficient is likely associated with an increase in radiative recombination of nonequilibrium charge carriers at elevated temperatures. Such behavior indicates a competition between optical absorption and recombination processes, with the latter becoming more significant as temperature rises.

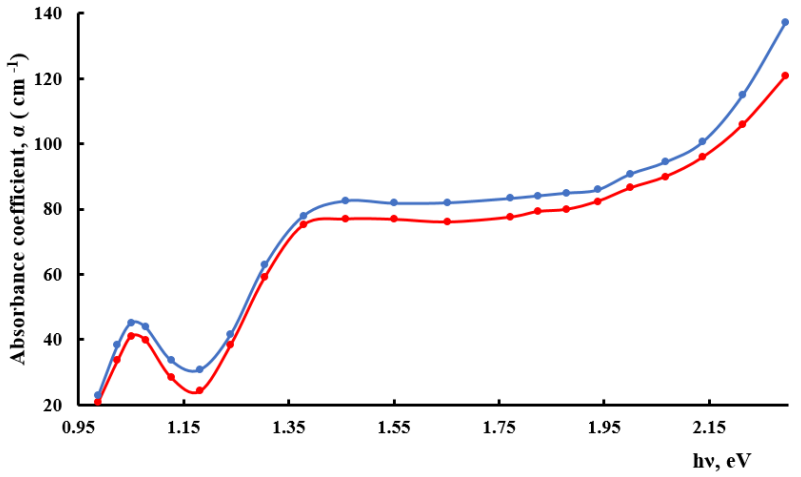

Fig. 4. Absorption spectra of the $Ga_{0.997}B_{0.003}Se$ crystal at 300 K (1) and 110 K (2)

To establish a more complete understanding of the optical response of boron-doped GaSe crystals, the spectral dependence of photocurrent for $Ga_{1-x}B_xSe$ (x = 0.3% and 0.5%) was measured at 295 K (Fig. 5). For $Ga_{0.997}B_{0.003}Se$ (Fig. 5a), the spectral shape changes considerably: the dominant photocurrent peak appears at 1.77 eV, while the long-wavelength edge extends to about 0.9 eV. This red-shift of the principal maximum relative to the fundamental absorption edge (≈ 1.96 eV) reflects the activation of boron-induced acceptor levels, which enable transitions of thermally excited electrons from localized states to the conduction band. The broadening of the spectral response further suggests the involvement of defect-related states in the photo generation process. For $Ga_{0.995}B_{0.005}Se$ (Fig.5b), the main photocurrent peak shifts slightly toward higher energy (≈ 1.95 eV) and the overall photocurrent amplitude decreases. This trend can be attributed to enhanced radiative recombination and a partial reduction in the density of localized impurity states at higher boron concentration. The observed spectral behavior indicates a competition between optical absorption and carrier recombination processes, consistent with the temperature-dependent absorption characteristics discussed earlier.

Overall, the close correspondence between the absorption edge (~ 1.96 eV) and the photocurrent maxima confirms that boron incorporation modifies both the optical and electrical photo response of GaSe in a correlated manner. Such correlation between absorption and photoconductivity spectra provides deeper insight into the role of boron-induced impurity levels in determining the carrier excitation and recombination mechanisms, thus supporting the potential of $Ga_{1-x}B_xSe$ crystals for broadband photodetector applications.

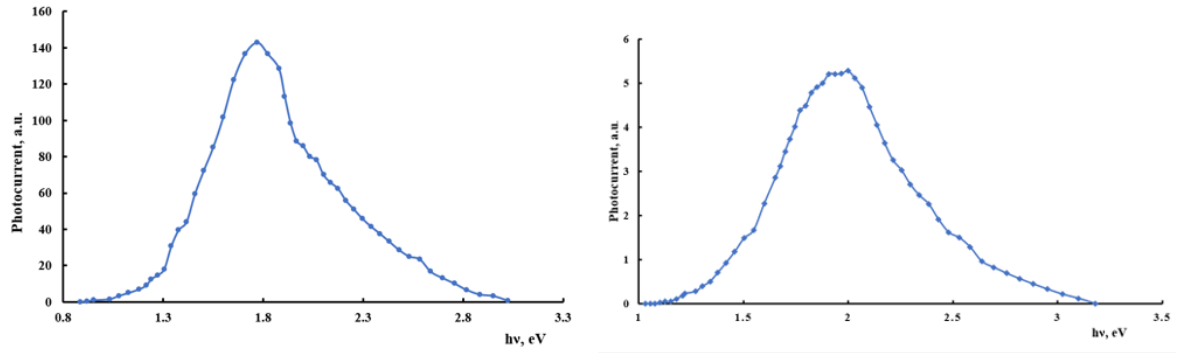

a) **b)**

Fig. 5. Photoconductivity spectra of $Ga_{1-x}B_xSe$ single crystals at 295 K: (a) x = 0.3% and (b) x = 0.5%.

4. Conclusion

In this study, single crystals of $Ga_{1-x}B_xSe$ (x = 0.3% and 0.5%) were successfully synthesized by the horizontal Bridgman method, and their optical and photoelectrical properties were systematically investigated. The incorporation of boron into the GaSe lattice led to distinct modifications in the electronic band structure and photo response behavior. UV–Vis absorption studies revealed a slight narrowing of the direct band gap from 2.0 eV for pure GaSe to approximately 1.960–1.963 eV for boron-doped samples, which effectively extended the optical absorption edge toward the longer-wavelength (visible–NIR) region. This band gap tuning occurred without degradation of crystalline quality, demonstrating that boron doping provides an effective means for tailoring the spectral sensitivity of GaSe-based materials. The appearance

of additional absorption features at 1.05 eV and 1.35 eV indicated the formation of boron-induced impurity states within the band gap. These localized levels were found to play a crucial role in determining the temperature-dependent optical behavior — at lower boron content, the absorption coefficient increased with temperature due to thermal excitation of carriers, whereas at higher boron concentration, enhanced radiative recombination resulted in a negative temperature coefficient of absorption. Photoconductivity measurements further confirmed the close relationship between the optical absorption and carrier excitation processes. The photocurrent spectra exhibited a strong peak at 1.77 eV for $Ga_{0.997}B_{0.003}Se$ and at 1.95 eV for $Ga_{0.995}B_{0.005}Se$, consistent with the absorption edge obtained from optical measurements. The red-shift and spectral broadening observed in the lower-doped sample reflected transitions involving boron-related acceptor levels and defect states, while the blue-shift and reduced amplitude at higher doping indicated increased recombination losses. These results clearly demonstrate a strong correlation between the optical absorption and photoconductivity spectra, highlighting the impact of boron incorporation on carrier generation and recombination mechanisms.

Overall, the findings confirm that controlled boron substitution provides an efficient approach for engineering the band structure and photo response of GaSe without compromising its layered crystalline nature. The combined optical and photoconductivity analyses reveal that $Ga_{1-x}B_xSe$ crystals possess tunable optoelectronic characteristics, making them highly promising materials for broadband photodetectors and other next-generation optoelectronic devices operating in the visible and near-infrared spectral regions.

REFERENCE LIST

26. Bastow, T. J., Campbell, I. D., & Whitfield, H. J. (1981). A 69Ga, 115In NQR study of polytypes of GaS, GaSe and InSe. Solid State Communications, 39(2), 307-311.
27. He, Z., Guo, J., Li, S., Lei, Z., Lin, L., Ke, Y., ... & Zhang, X. (2020). GaSe/MoS2 heterostructure with ohmic-contact electrodes for fast, broadband photoresponse, and self-driven photodetectors. Advanced Materials Interfaces, 7(9), 1901848.
28. Abderrahmane, A., Jung, P. G., Kim, N. H., Ko, P. J., & Sandhu, A. (2017). Gate-tunable optoelectronic properties of a nano-layered GaSe photodetector. Optical Materials Express, 7(2), 587-592.
29. Hu, P., Wen, Z., Wang, L., Tan, P., & Xiao, K. (2012). Synthesis of few-layer GaSe nanosheets for high performance photodetectors. ACS nano, 6(7), 5988-5994.
30. Curreli, N., Serri, M., Zappia, M. I., Spirito, D., Bianca, G., Buha, J., ... & Bonaccorso, F. (2021). Liquid-phase exfoliated gallium selenide for light-driven thin-film transistors. Advanced Electronic Materials, 7(3), 2001080.
31. Kumar, A. S., Wang, M., Li, Y., Fujita, R., & Gao, X. P. (2020). Interfacial Charge Transfer and Gate-Induced Hysteresis in Monochalcogenide InSe/GaSe Heterostructures. ACS Applied Materials & Interfaces, 12(41), 46854-46861.
32. Tao, H., Fan, Q., Ma, T., Liu, S., Gysling, H., Texter, J., ... & Sun, Z. (2020). Two-dimensional materials for energy conversion and storage. Progress in Materials Science, 111, 100637.
33. Ertap, H. (2018). Nonlinear absorption, SHG behavior and carrier dynamics of Nd and Pr doped GaSe single crystals. Optical Materials, 83, 99-103.
34. Bassou, A., Rajira, A., El Kanouny, A., Abounadi, A., El Haskouri, J., & Almaggoussi, A. (2021). Optical properties of GaSe, characterization and simulation. Materials Today: Proceedings, 37, 3789-3792.
35. Zalamai, V. V., Stamov, I. G., & Syrbu, N. N. (2021). Interference of exciton-polariton waves in GaSe nanocrystals. Materials Today Communications, 27, 102355.

36. Wu, Y., Fuh, H. R., Zhang, D., Coileáin, C. Ó., Xu, H., Cho, J., ... & Wu, H. C. (2017). Simultaneous large continuous band gap tunability and photoluminescence enhancement in GaSe nanosheets via elastic strain engineering. Nano Energy, 32, 157-164.
37. Bassou, A., Rajira, A., El-Hattab, M., El Haskouri, J., Murcia-Mascaros, S., Almaggoussi, A., & Abounadi, A. (2022). Structural and optical properties of a layered ε-GaSe thin film under elastic deformation from flexible PET substrate. Micro and Nanostructures, 163, 107152.
38. Huang, L., Chen, Z., & Li, J. (2015). Effects of strain on the band gap and effective mass in two-dimensional monolayer GaX (X= S, Se, Te). Rsc Advances, 5(8), 5788-5794.
39. Ma, Y., Dai, Y., Guo, M., Yu, L., & Huang, B. (2013). Tunable electronic and dielectric behavior of GaS and GaSe monolayers. Physical Chemistry Chemical Physics, 15(19), 7098-7105.
40. Rybkovskiy, D. V., Arutyunyan, N. R., Orekhov, A. S., Gromchenko, I. A., Vorobiev, I. V., Osadchy, A. V., ... & Obraztsova, E. D. (2011). Size-induced effects in gallium selenide electronic structure: The influence of interlayer interactions. Physical Review B—Condensed Matter and Materials Physics, 84(8), 085314.
41. Lei, S., Ge, L., Liu, Z., Najmaei, S., Shi, G., You, G., ... & Ajayan, P. M. (2013). Synthesis and photoresponse of large GaSe atomic layers. Nano letters, 13(6), 2777-2781.
42. Wang, C., Yang, S. X., Zhang, H. R., Du, L. N., Wang, L., Yang, F. Y., ... & Liu, Q. (2016). Synthesis of atomically thin GaSe wrinkles for strain sensors. Frontiers of Physics, 11(2), 116802.
43. Wang, Z., Wei, X., Huang, Y., Zhang, J., & Yang, J. (2023). High solar-to-hydrogen efficiency in AsP/GaSe heterojunction for photocatalytic water splitting: A DFT study. Materials Science in Semiconductor Processing, 159, 107393.
44. Li, X., Bao, A., Guo, X., Ye, S., Chen, M., Hou, S., & Ma, X. (2023). A type-II GaP/GaSe van der Waals heterostructure with high carrier mobility and promising photovoltaic properties. Applied Surface Science, 618, 156544.
45. Bassou, A., Rajira, A., Gil, B., Almaggoussi, A., & Abounadi, A. (2023). Accurate determination of optical parameters of non transparent materials: The ε–GaSe case. Optical Materials, 140, 113887.
46. Kępińska, M., Nowak, M., Duka, P., & Kauch, B. (2009). Spectrogoniometric determination of refractive indices of GaSe. Thin Solid Films, 517(13), 3792-3796..
47. Chen, Y., Sun, Y., Dai, X., Zhang, B., Ye, Z., Wang, M., & Wu, H. (2015). Tunable electrical properties of NiO thin films and p-type thin-film transistors. Thin Solid Films, 592, 195-199.
48. Garcés, F. A., Budini, N., Arce, R. D., & Schmidt, J. A. (2015). Effect of thickness on structural and electrical properties of Al-doped ZnO films. Thin solid films, 574, 162-168.
49. Muydinov, R., Steigert, A., Schönau, S., Ruske, F., Kraehnert, R., Eckhardt, B., ... & Szyszka, B. (2015). Water-assisted nitrogen mediated crystallisation of ZnO films. Thin Solid Films, 590, 177-183.
50. Wang, Y., Capretti, A., & Dal Negro, L. (2015). Wide tuning of the optical and structural properties of alternative plasmonic materials. Optical Materials Express, 5(11), 2415-2430.
51. Pankove, J. I. (1971). Optical processes in semiconductors Prentice-Hall. New Jersey, 92, 36.
52. Andres-Penares, D., Cros, A., Martinez-Pastor, J. P., & Sanchez-Royo, J. F. (2017). Quantum size confinement in gallium selenide nanosheets: band gap tunability versus stability limitation. Nanotechnology, 28(17), 175701.
53. Guseinov, A. G., Salmanov, V. M., Mamedov, R. M., Salmanova, A. A., & Akhmedova, F. S. (2017). Optical Properties of Boron-Doped Gallium Selenide. Optics and Spectroscopy, 123(6), 875-880.
54. Agekyan V.F., Grigorieva N.R. (2016). Luminescence of semiconductor crystals. St. Petersburg: Publishing house of St. Petersburg University, 2016. 156 p.